INTERNATIONAL ATOMIC ENERGY AGENCY
UNITED NATIONS EDUCATIONAL, SCIENTIFIC AND CULTURAL ORGANIZATION
INTERNATIONAL CENTRE FOR THEORETICAL PHYSICS
I.C.T.P., P.O. BOX 586, 34100 TRIESTE, ITALY, CABLE CENTRATOM TRIESTE

SMR.703 - 2

WORKING PARTY ON:
MECHANICAL PROPERTIES OF INTERFACES

23 AUGUST - 3 SEPTEMBER 1993

"Basic and Introductory Lectures on Fracture" (Part II)

"Lattice Imperfections by Lattice Green's Functions"

Robb THOMSON
United States Department of Commerce
National Institute of Standards and Technology
Materials Science and Engineering Laboratory
Building 223
Gaithersburg, MD 20899
U.S.A.

Lattice Imperfections by Lattice Green's Functions

Robb Thomson

Laboratory for Materials Science and Engineering

National Institute of Standards and Technology

Technology Administration

US Department of Commerce

Gaithersburg, MD 20899

S. J. Zhou and A. E. Carlsson

Department of Physics

Washington University

St Louis, MO 63130

V. K. Tewary

Materials Reliability Division

National Institute of Standards and Technology

Technology Administration

US Department of Commerce

Boulder, CO 80303

(Received)

This paper explores the use of lattice Green's functions for calculating the static structure of defects in lattices, in that the atoms of the lattice interact with their neighbors with an arbitrary nonlinear (short range) potential. The method is hierarchical, in which Green's functions are calculated for the perfect lattice, for increasingly complicated defect lattices, and finally the nonlinear structure problem is iterated till a converged solution is found. For the case where the defect must be embedded within a very large linear system, and the slip plane, cleavage plane, nonlinear zone, etc. can be made small compared to the system size, Green's functions are a very powerful method for studying the physics of defects and their interactions. As an illustration of the method, we report numerical calculations for an interfacial crack emitting dislocations from an interface between two joined 2D hexagonal lattices. The supercell size was 4×10^6, and the crack length was 101 lattice spacings. After the Green's functions were obtained for the defective lattice, the dislocation and crack structures were obtained in a minute or less, making possible detailed studies of the defects with various external loads, force laws, defect relative positions, etc. with negligible computer time. With practical supercomputer times, supercell and defect sizes one or two orders larger are feasible, thus making possible realistic calculation of 3D nucleation events on cracks, etc.

Typeset Using *REVTEX*

I. INTRODUCTION

The purpose of this paper is to demonstrate, and in part to recall, the use of lattice Green's functions in the study of the structure and quasi-static properties of imperfections in lattices, and to show that for many uses, the method outlined is superior to other numerical techniques for simulating defects in lattices. We will illustrate this point in the specific case of cracks and dislocations in a 2D hexagonal lattice. The method begins with the computation of the perfect lattice Green's function, then calculates the Green's function for the imperfection in the harmonic approximation, and lastly deduces the final structure from non-linear force laws by a relaxation technique.

The method described here builds on earlier work by Kanzaki[1] on lattice statics and Tewary[2, 3] on Green's-function methods. Our motivation for using these methods, rather than the direct simulation methods that are more widely used today, is the prospect for studying very large systems in 3D, with the order of $10^7 - 10^8$ atoms. The system size is important for cracks and dislocations, in part because of the long range character of the strain fields ($1/r$ in the case of the dislocation and $1/\sqrt{r}$ in the case of the crack), and in part because nucleation events for cracks and dislocations require fully 3D computation. In the other methods, the much more limited size of the possible systems which can be studied brings into play serious difficulties with the boundary conditions on the surfaces, or at the junction of the periodic supercells in infinite systems. In addition, localized lattice defects like cracks and dislocations are ideally suited to the Green's function approach because the nonlinear part of the problem is relatively localized, and the long range strain is quite accurately linear. This feature allows us to treat the nonlinear aspects of the problem in a very efficient manner.

In our early work[4–7], we largely restricted ourselves to a very simple lattice

which we have called "atoms on rails". This lattice is a simple cubic (2D or 3D) in which displacements are only allowed in one direction. In this lattice, we worked out a number of qualitative examples illustrating the behavior of cracks. However, this lattice has a serious defect in that the continuum analogue of the lattice does not have a symmetric stress tensor. After the early stages of our own work, done initially with "snapping" linear bonds[4], Esterling[8] pointed out how to address nonlinear problems in lattice statics. Finally, Tewary, et al[9] have demonstrated how to handle interfaces in a general manner.

II. GENERAL RELATIONS.

Here we follow the treatment of Tewary[3]. The force constant operator, $\Phi_{ij}(\mathbf{l}, \mathbf{l}')$, or "dynamical matrix"[10] is defined as an appropriate second derivative of the total strain energy of the lattice, and is the force exerted in the i direction on an atom at the lattice point, $\mathbf{l}$, by an atom at the lattice point $\mathbf{l}'$ as the latter is displaced a unit distance in the j direction. This harmonic spring force on a reference atom located at $\mathbf{l}$ caused by the displacements of its neighbors (or itself) must be balanced by an external force, $\mathbf{F}$, applied to the atom, as given in the equation,

$$\phi_{ij}(\mathbf{l}, \mathbf{l}')u_j(\mathbf{l}') = -F_i(\mathbf{l}) \tag{2.1a}$$

$$\Phi\mathbf{u} = -\mathbf{F} \tag{2.1b}$$

In this and all subsequent equations, the summation over repeated indices is implied. The displacements of the reference atom and its neighbors is given by $u_j(\mathbf{l}')$. The negative sign on the right expresses our force sign convention—i.e. all forces are positive when exerted on the atom in question. The lattice is shown schematically in Fig. 1. In case the lattice contains a basis, with more than one atom per primitive cell, then we will assume this basis is included in the direction indices, (i, j). Thus,

if there is one atom per cell, $(i,j = 1,2,3)$, whereas if there are two atoms, then $(i,j = 1-6)$, etc. Eqn. (2.1b) is written in the operator form.

A number of general relations on the force constant matrix follow from lattice symmetry and other requirements[10], and the most useful of them is the expression of Newton's third law,

$$\sum_{l'} \phi_{ij}(l,l') = 0. \tag{2.2}$$

Keating's theorem (the invariance of the potential function to rotation of the lattice requires that the strain energy must be expressible as a function of dot products of relative atomic displacements) makes possible a considerable simplification in the complex lattices[11].

By definition, the Green's function operator is (in our case the negative of) the inverse of the force constant operator,

$$\Phi^{-1} = -\mathbf{G} \tag{2.3a}$$

$$\mathbf{u} = \mathbf{GF} \tag{2.3b}$$

The second of these equations expresses the formal solution of the problem of finding the lattice displacements, if the applied external forces are known. In the perfect lattice, where $\phi_{ij}(l',l) = \phi_{ij}(l-l')$ and $g_{ij}(l,l') = g_{ij}(l-l')$, because of the lattice translation symmetry, G is easily obtained in k-space,

$$\phi_{ij}(l-l') =$$

$$\tfrac{1}{8\pi^3 N^3} \textstyle\sum_{B\ zone} \phi_{ij}(\mathbf{k}) \exp(-i\mathbf{k}(l-l')) \tag{2.4a}$$

$$\phi_{ij}(\mathbf{k}) = \textstyle\sum_{shell} \phi_{ij}(l-l') \exp(i\mathbf{k}(l-l')) \tag{2.4b}$$

where $\phi_{ij}(\mathbf{k})$ is understood to be the transform function of $\phi_{ij}(l-l')$, and B zone denotes the Brillouin zone.. In these equations, we have assumed Born-von Karman

periodic boundary conditions (Fig. 1) with periodicity N in each direction. The "atoms on rails" simple cubic lattice noted in the Introduction, is one special case where the limit $\to \infty$ can be made, because one of the integrations over the B-zone is analytic[4]. Formally, the sum over the "shell" is a sum over the Born-von Karman supercell, but because the forces between atoms are always short ranged (Coulomb forces have to be dealt with separately), the sum in Eqn. (2.3b) is actually only over the region within the shell of atoms defined by the range of the force.

The Green's function operator has a similar Fourier expansion, and the inversion of ϕ is simply

$$\begin{aligned} g_{ij}(\mathbf{k}) &= [\phi_{ij}(\mathbf{k})]^{-1} \\ &= \left[\sum_{shell} \phi_{ij}(l-l') \exp(i\mathbf{k}(l-l'))\right]^{-1} \end{aligned} \tag{2.5}$$

Since in 3D, ϕ is a 3x3 (or 3n×3n matrix, where n is the number of atoms in the lattice basis), the right side of (2.5) requires the inversion of a small matrix for each value of k. Noting that $\phi_{ij}(\mathbf{k})$ in Eqn. (2.5) is the sum over the shell of atoms within the range of the force law, the perfect lattice G's are easily determined, numerically. When the inverse Fourier transform is performed on the $g_{ij}(\mathbf{k})$, then the Green's function operator in real space, $\mathbf{g}_{ij}(l-l')$, is determined. In 2D, the normalization constant in front of the summation in Eqn. (2.4a) is replaced by $1/(4\pi^2 N^2)$.

Although the analysis to this point seems benign, there is an important subtlety in the physics which needs to be clarified. Strictly speaking, the Green's function operator we have defined gives the response to a unit point force source, and the lattice is thus subjected to a net force. It is consequently not in static equilibrium. This anomaly is connected to the fact that $g_{ij}(\mathbf{k})$ is singular at the point $\mathbf{k} = 0$, and in the continuum limit, $g(l)$ is logarithmically divergent. Although one could set up the analyis for a dipole source with no net force[4], it will be more straight

forward to have an analysis representing a single force, and we will in this case simply delete the singular term in the Brillouin sums at $\mathbf{k} = 0$. This stratagem is permitted because when the balancing forces are added during the solution of the total problem, the singular terms exactly cancel—that is, the singular term does not depend on the lattice position. What results is a Green's function which, in 2D, has a logarithmic asymptotic form, and depends explicitly on the density of points in k-space, reflecting the logarithmic singularity at the origin. When the actual (net zero) forces are finally applied to the lattice, these artifacts are removed, and physical results are generated which are independent of the size of the supercell for large supercells.

A similar requirement pertains to the conservation of angular momentum. In this case, when torques result from the application of forces on atoms in the system (normally applied to atoms near the center of a supercell), then cancelling torques will be required by adding small forces on the boundary of the supercell. In our experience, when the initial torque lever arm is small, and the supercell is large, we find that the results are altered only in a small way when the balancing torques are applied. Thus the zero-torque requirement can safely be ignored.

At this point in the analysis, a set of perfect lattice Green's functions have become available in real space coordinates. It is then necessary to address the imperfect lattice, Fig. 2. We will treat imperfections in the lattice via changes in the couplings between the atoms, such as for example bond-cutting at a crack. When the number of altered sites is a minority of the sites in the lattice, a straightforward approach offers itself through the Dyson equation. That is, we consider changes, $\delta\Phi$, in the springs connecting the perfect lattice, and write the defining equation for the Green's function in the altered lattice,

$$(\Phi + \delta\Phi)\mathbf{G}^* = -\mathbf{1} \tag{2.6}$$

where the star represents the Green's function for the lattice containing a defect. Now we multiply (2.6) on the left by the Green's function operator for the perfect lattice and obtain the Dyson equation

$$(\mathbf{1} - \mathbf{G}\delta\Phi)\mathbf{G}^* = \mathbf{G}, \tag{2.7}$$

from which

$$\mathbf{G}^* = \mathbf{G}(\mathbf{1} - \delta\Phi\mathbf{G})^{-1} \tag{2.8}$$

If both arguments of $\mathbf{G}^*$ are in the defect subspace, then in Eqn. (2.8) only the piece of $\mathbf{G}$ involving this subspace is needed. This piece, as well as $\delta\Phi$, are matrices whose order is equal to the number of degrees of freedom in the defect subspace. Thus one simply has to perform a simple matrix inversion, and then multiplication, to obtain $\mathbf{G}^*$ in the defect subspace. To obtain $\mathbf{G}^*$ outside the defect subspace, one expands Eqn. (2.8) as follows [12]:

$$\mathbf{G}^* = \mathbf{G} + \mathbf{G}\delta\Phi\mathbf{G} + \mathbf{G}\delta\Phi\mathbf{G}\delta\Phi\mathbf{G} + \cdots \tag{2.9}$$

This gives the exact relation

$$\mathbf{G}^* = \mathbf{G} + \mathbf{G}\mathbf{T}\mathbf{G} \tag{2.10}$$

where

$$\mathbf{T} = \delta\Phi[\mathbf{1} - \mathbf{G}\delta\Phi]^{-1}. \tag{2.11}$$

Here, $\mathbf{T}$, $\mathbf{1}$, and $\mathbf{G}$ are considered as $3n$ by $3n$ matrices acting in the defect subspace ($2n$ by $2n$ in 2D). Thus the basic mathematical operation is simply the inversion of a finite-dimensional matrix.

The Dyson equation has a particularly useful pictorial representation in terms of a "Feynman" diagram, as shown in Fig. 3. The product, $\mathbf{G}\delta\Phi\mathbf{G}^*$ in (2.7) represents

in scattering theory a propagator $\mathbf{G}^*$ (heavy directed line) from the source point l′ to the intermediate point l‴, where it is scattered (wavy line) by $\delta\Phi$ to the second intermediate point, l″, where the propagator G (directed line) takes the process to the final field point, l. We will use the heavy line, wavy line, etc. notation in subsequent figures without designating G, $\delta\Phi$, etc. for clarity in the diagrams. This pictorial representation is quite useful in writing down the detailed operators, because one can easily check that all the paths leading from a specific initial point to a specific final point have been accounted for via all the necessary "scattering" events. In the special case of pair force bonds, the annihilation of a bond involves two diagrams for each of the two atoms connected by the bond. Fig 3a depicts a "scattering" due to the force that displacement of one atom causes in the other, while Fig 3b shows the effect that displacement of an atom has on itself. By Newton's third law (Eqn. (2.2)), $\delta\Phi$ for the two cases are the negative of each other.

The final step in finding the structure of the defect is to move out of the harmonic world into the final nonlinear one. Here the underlying principle is that the sum of all the forces acting on each atom must vanish, that is, from Eqn. (2.1b),

$$\mathbf{F} + \mathbf{f} + \Phi^*\mathbf{u} = 0. \tag{2.12}$$

Here, Φ^* is the spring constant operator in the defective lattice. F are the known externally applied forces, and f are the forces which are exerted by atoms whose bonds may be stretched into their nonlinear regimes. They include all the higher order anharmonic terms in the potential energy. These latter nonlinear bonding forces, are, by definition, not a part of the linear part of the problem, and the atoms which contribute such forces are removed from the problem, and placed in the defect space during the construction of the linear system, described by the Green's function, $\mathbf{G}^*$. In the nonlinear problem, the atoms in the defect space and their nonlinear bond

forces are added back into the problem, in a formal way, as "external" forces. When Eqn. (2.12) is multiplied on the left by $\mathbf{G}^*$, we obtain

$$\mathbf{u} = \mathbf{G}^*\mathbf{F} + \mathbf{G}^*\mathbf{f}\{\mathbf{u}\} \tag{2.13}$$

In this equation, we have highlighted the special character of the nonlinear bonds by identifying them with a specified force law, $\mathbf{f} = \mathbf{f}\{\mathbf{u}\}$, where f is a functional of the positions of the atoms in the vicinity of the reference atom. If the displacements, u can be made everywhere consistent with the forces in the nonlinear bonds so that (2.13) is satisfied, then the problem of the lattice structure of the defect is solved.

To summarize, the defect subspace is constructed in order to accomodate a set of nonlinear bonds, and additional bonds may have to be annihilated to form free surfaces, etc. After the necessary defect Green's functions, $\mathbf{G}^*$, are constructed from the Dyson equation, the nonlinear bonds are reattached to atoms in the cohesive zone portion of the defect subspace, and the nonlinear set of equations, (2.13), are solved for the atoms in the cohesive zone. The true external forces, F, may be applied to atoms either within or without the defect subspace.

Eqn. (2.13) is a set of nonlinear equations, to be solved by an iterative relaxation technique. Their number is pn where n is the number of atoms to which nonlinear bonds are attached, and p is the dimensionality of the problem. It is necessary to introduce damping in the process, otherwise the solutions generally gyrate wildly when the trial is not close to final convergence. That is, if $\mathbf{u}^{(1')}$ is the new solution on the left generated from a trial function, $\mathbf{u}^{(0)}$, on the right side of (2.13), and if $\delta = \mathbf{u}^{(1')} - \mathbf{u}^{(0)}$, then the new trial solution is taken to be $\mathbf{u}^{(1)} = \mathbf{u}^{(0)} + \epsilon\delta$, where ϵ is a small number, optimized by trial and error.

The reader may be puzzled that we have used an equation, (2.13), which is apparently valid only in the linear regime, to solve a nonlinear problem. The method, is

nevertheless completely rigorous, because any set of "external" forces, **f**, can be specified on the right side of (2.13). By trial and error, the iteration proceedure simply finds that set which is consistent with a specified (nonlinear) force law.

Equation (2.13) is the discrete analogue to the Barenblatt integral equation for a distribution of cohesive forces in the continuum approximation[13].

At this point, it is necessary to make two general comments about the method. The first concerns the overall accuracy of the method. Once one has iterated Eqn. (2.13) to convergence the remaining inaccuracies in the method come from treating the forces outside the nonlinear region as being perfectly harmonic. Since one often finds displacements many times larger than a lattice parameter, this might appear to be a questionable assumption. However, it is not the absolute displacement which is important, but the displacements relative to other atoms in the force shell, which must be small compared to a lattice parameter. That is, the Green's function analysis is a small strain theory.

The second point concerns a complexity involving the cutting of bonds in problems like the crack. If the force laws extend beyond the first neighbor shell, then the springs to the first coordination shell will often be in compression, while the springs to the second are in tension, and so forth. In the expansions of the potential functions for the harmonic lattice, these forces do not appear, because the lattice is expanded about its equilibrium position, and the symmetry of the lattice cancels out such forces. But, in the Dyson equation analysis, when bonds are cut, the lattice symmetry is destroyed, and these forces must be accounted for, explicitly, on the right side of Eqn. (2.13) as additional constant forces at the appropriate lattice sites. In Tewary's paper[2], he has dealt with these terms in a different, and more formal, way than we have here. These forces are also discussed in the first chapter of Maradudin, etal[10].

III. INTERFACES.

Tewary, etal[9] have demonstrated how to incorporate an infinite interface into the analysis, and we will briefly repeat and extend their argument here using the point of view and terminology of this paper.

The central idea is that the imperfect lattice with the interface will generally be periodic for translations parallel to the interface, but it will not be periodic in directions normal to the interface. This property allows us to introduce a mixed representation into the ϕ and g at the Dyson equation stage, $\phi_{ij}(k_x, k_y; l_z, l'_z)$, which again projects the Dyson equation into the defect subspace corresponding to the single coordinate, z, normal to the surface. We will arrive at interfacial Green's functions by first constructing free surface functions, and then gluing two half spaces together to form the interface. The mixed-basis bond-cutting method for obtaining the surface Green's functions is quite similar to that used by Kalkstein and Soven[15] for electronic Green's functions; Dobrzynski et al[16] have subsequently calculated electronic Green's functions for interfaces using a "gluing" method.

In Fig. 4, we show a schematic drawing of the Born–von Karman periodic solid with a cut through the middle of a supercell. The lattice is then separated at the cut into two non–interacting parts. Because of the periodicity, if a cut is made in one supercell, this cut is also automatically repeated in every other supercell above and below the cut in question. Thus, a disconnected set of slabs is created, each with thickness equal to the supercell length, N. Thus, it is possible to deal with a single slab as the total system. In such a construction, the number of cut bonds within one of the supercells is of order N^2 (in 3D), and the defect sub–space is not small, as assumed in the previous section. However, if the cut is made in a symmetry direction of the lattice, then, the lattice points contained in the cut constitute a periodic 2D array, and all quantities, ϕ, g, etc. for the defect sub–space are periodic

in the coordinates contained within the cut. No quantities are, of course, periodic in the direction normal to the cut.

For the sake of simplicity of argument, a cubic 3D lattice, with a cut on the [001] plane is assumed. Consequently, just as in the perfect lattice, in the x and y directions, all quantities in the slab may be written in the form $\phi_{ij}(l_x - l'_x, l_y - l'_y; l_z, l'_z)$, etc. After all quantities in the x and y directions are converted to the mixed representation alluded to above, then, following the steps leading to the Dyson equation, (2.7), one finds

$$(\delta_{ik}\delta_{l_z,l''_z} - g_{im}(k_x, k_y; l_z, l'''_z)\delta\phi_{mk}(l'''_z, l''_z)) \times g^*_{kj}(k_x, k_y; l''_z, l'_z) = g_{ij}(k_x, k_y, l_z - l'_z) \qquad (3.1)$$

Note that $\delta\phi$ is only a function of the z-coordinate, and does not depend on x and y. This equation is now a set of linear equations for the different lattice points, l_z contained in the defect sub-space, that is for the lattice points on the surface where the bonds have been cut.

However, it is important to straighten out one issue here, which is the interpretation of l''_z and l'_z in g^*. Since there is a l''_z and a l'_z layer in each slab, it is not immediately obvious precisely which pair of l''_z and l'_z layers g^* refers to. The answer is that g^* always refers to the l''_z and l'_z layers inside the same slab. Depending on the partitioning of the system into unit cells (which have the same thickness as the slabs but are not necessarily identical to them), this may mean that g^* actually describes connections between different unit cells. This happens, for example, if the edges of the unit cells are placed at the centers of the slabs, which is sometimes a convenient geometry. In this case, if l''_z is at the top of a slab, and l'_z is at the bottom, then g^* describes not the connection between the top of one slab and the bottom of the above slab (which might seem to be the obvious interpretation), but rather the connection

between the top and bottom of the same slab. Because of this connection, the Green's functions for the finite slab are different from those for a semi-infinite half space. If the size of the supercell, N, is large, the numerical difference will of course be quite small. It may seem surprising that g^*, which is built up of quantities that have periodicity N (which equals the slab thickness) can exactly describe properties of a single slab. This is made possible by the fact that the slabs are noninteracting after the bonds are cut, which makes the artificial slab-to-slab periodicity irrelevant. These points are illustrated in Fig. 5 where the Feynman diagrams for the slab construction are shown.

We note that the rank of the Dyson equation for the slab may be quite small, since the x and y coordinates are not in the problem. For example, if n bonds per unit cell are annihilated at the surface, and if $(i, j = 1, 3)$, then the slab Dyson equation has rank $(6n)$. (Remember that both upper and lower slab surfaces must be included.) If they are needed, the slab Green's functions in real space may be found by taking the Brillouin sum over the appropriate cut in (k_x, k_y) space.

If it is desired to obtain interfacial Green's functions, then it is necessary to take the additional step of gluing two slabs (characterized by different spring constants) together, Fig. 4b. Still working in the mixed representation of Eqn. (3.1), the bonds which were cut in constructing the slab are reconnected (with a third spring constant between the two slabs).

The new Dyson equation for the interface has exactly the same form as (3.1),

$$(\delta_{ij}\delta_{l_z,l''_z} - g_{im}(k_x, k_y; l_z, l'''_z)\delta\phi_{mk}(l'''_z, l''_z)) \times g^*_{kj}(k_x, k_y; l'''_z, l'_z) = g_{ij}(k_x, k_y, l_z - l'_z) \qquad (3.2)$$

In this equation, the g^* are the interface Green's functions, and the g's are the slab Green's functions, calculated in (3.1). There are, however, two sets of g's, one for an

upper slab, (b), characterized by one set of spring constants, and another for a lower slab, (a), characterized by a second set of spring constants. (A separate notation for the slab Green's functions has not been introduced, in order to retain a tidy Eqn. (3.2)). The reader must simply remember that slab g's are constructed from perfect lattice g's, interface g's are constructed from slab g's, etc.) In contrast to the slab construction, in the interface construction, the two slabs are joined at only one interface, and atoms on the upper surface of one slab are connected to atoms on the lower surface of the second slab. Thus, the interface Dyson equation, (3.2), has rank only (3n). If the slabs are joined at both edges, one would instead obtain a long-period (a)-(b) superlattice.

Fig. 6 shows the Feynman diagram for the interface Dyson equation.

The interface Green's functions which result from the solution of the interface Dyson equation are again in mixed representation, and must be converted to the full real space representation by performing the Brillouin sum over the (k_x, k_y) cut. The interface Green's functions will be functions of three sets of parameters: elastic constants in slab (a), elastic constants in slab (b), and spring constants connecting the two slabs. In practice, these constants can be normalized to one of the slabs, say (a), so that only two sets of parameters are involved. The Green's functions must be recalculated for every choice of these parameters.

Once the interface Green's functions have been obtained, then cracks and other defects can be studied as before. That is, the crack must be made by cutting a finite number of bonds on the interface, etc., new crack Green's functions constructed, and so forth. We have described a staged process: One starts with a perfect lattice Green's function, constructs as many levels of defect sub–spaces as are necessary, and then finally solves the indicated non linear problem in Eqn. (2.13) with the the Green's functions constructed from the highest level defect sub–space.

IV. 2D HEXAGONAL LATTICE.

In the following, the formal analysis of the previous sections will be illustrated by applying it to a crack in a hexagonal 2D lattice, Fig. 7. The lattice is bonded by springs connected only to nearest neighbors with central forces. If the spring constant is α, then the individual ϕ matrices are given by

$$\phi(10) = \alpha \begin{pmatrix} 1 & 0 \\ 0 & 0 \end{pmatrix} = \phi(\bar{1}0) \tag{4.1a}$$

$$\phi(01) = \frac{\alpha}{4} \begin{pmatrix} 1 & \sqrt{3} \\ \sqrt{3} & 3 \end{pmatrix} = \phi(0\bar{1}) \tag{4.1b}$$

$$\phi(\bar{1}1) = \frac{\alpha}{4} \begin{pmatrix} 1 & -\sqrt{3} \\ -\sqrt{3} & 3 \end{pmatrix} = \phi(1\bar{1}) \tag{4.1c}$$

$$\phi(00) = -\alpha \begin{pmatrix} 3 & 0 \\ 0 & 3 \end{pmatrix} \tag{4.1d}$$

The lattice sites in the matrix $\phi(l, l')$ are given in the units of the primitive hexagonal lattice cell, Fig. 7.

When the crack is made in the lattice, bonds are cut in the cleavage plane, as shown in Fig. 7. The crack Green's functions are obtained from the Dyson equation, (2.7). For each choice of field and source point, there is a sum to be carried out over all the cut bonds. We will discuss the calculation in terms of a sum over the various Feynman diagrams in the problem.

We have also studied a different configuration corresponding to a crack progressing to some point in the cohesive zone, and either emitting a dislocation on one of the planes at 60°, or cleaving on that plane. This configuration is shown in Fig. 8.

Finally, we have studied a crack on an interface between two hexagonal lattices. That is, the atoms below the cleavage plane in Fig. 7 are characterized by $\alpha = \alpha_1$ and those above by $\alpha = \alpha_2$. For bonds which cross the cleavage plane, $\alpha = \alpha_{12}$. There are two consecutive Dyson equations to solve, the first to make the slab, and the second

to connect two slabs to form the interface. As discussed in §III, both these Dyson equations are to be solved in the mixed representation.

After the appropriate Green's functions have been determined, the relaxation problem for the reconstituted bonds in the cohesive zone, Eqn.(2.10), is solved with force laws appropriate to the problem. We used the universal binding relation of Rose, etal[17], for the energy, U, in a bond between two atoms which have been stretched from equilibrium by amount u. In the following, we normalize all distances and displacements to the lattice spacing.

$$U = -\alpha\beta(u+\beta)\exp(-u/\beta) + C \tag{4.2a}$$

$$f = -\alpha u \exp(-u/\beta) \tag{4.2b}$$

Here, β is the range of the force law, and α is the linear spring constant term. In the first of these equations, C is a constant chosen to make U continuous at the cutoff distance, which is inside the second-neighbor distance. In the second, f is the force on an atom when its neighbor is given the displacement, u, along the radius vector between the two.

In Figs. 9-11 some results are shown for our calculations. Detailed discussion of the physical implications of the computer calculations will be presented in subsequent papers, but the figures illustrate the kind of results we have been able to obtain with the Green's function methodology. The parameters for the calculations were $N = 2 \times 10^3$; total length of crack line equals 101; length of cohesive zone at the crack tip where the bonds are reconstituted with the forces given by Eqn. (4.2b) in Figs. 9, 10 is 20.

In Fig. 9, we show the atoms in the cohesive zone at the right end of the crack where nonlinear bonds are attached. (These atoms correspond to the two atom pairs with wiggly bonds in Fig. 2.) The external load, **F**, for the system was a pair of

forces applied to the atoms at the center of the crack, see Fig. 2. Here, however, the force is composed of both tensile and shear components. In Fig. 9, the tensile force is sufficient to open the crack tip against the bonding forces which tend to close it. That is, the crack is loaded by a tensile force at its Griffith load. In addition, a shear component is added so that the atoms at the tip are sheared, and a dislocation is shown just before it is emitted from the crack core. The parameters in the universal binding curve, Eqn. (4.2b), were $\alpha = 1.0$, $\beta = 0.2$. In this calculation, the cleavage and dislocation emission are restricted to the cleavage plane of the crack. We call this a Mode II emission configuration. This crack was found to have very small lattice trapping of about 8%. The ratio of the critical stress intensity for emission relative to the Griffith stress intensity was 0.38. All these physical features change with the force law parameters. This configuration is particularly appropriate for studying the emission properties of cracks, and will be compared with both elastic[18] and quasi-elastic Peierls models[19] of the crack in subsequent papers.

In Fig. 10, the same phenomena are displayed for a crack on an interface between two hexagonal crystals. In this case, the displacements on top and bottom are no longer symmetric relative to one another, indicative of the elastic mismatch between the two lattices. We have chosen $\alpha_1 = 1.0$, $\alpha_2 = 2.0$, $\alpha_{12} = 0.5$ for the elastic constants, and in the interfacial force law, $\beta = 0.2$. The emission to Griffith load ratio is 0.2 for a positive shear and 0.6 for negative. In addition, the Griffith value decreases by about 12% in going from positive to negative emission, corresponding to an embrittlement under negative shear. (That is, the Mode I loading at Griffith equilibrium for positive Mode II emission is greater than that for negative emission.) The figure is shown for the configuration just before emission under positive shear. These results for interfaces suggest an interesting mechanism for interfacial embrittlement for interfaces between misfitting lattices, which will be pursued in subsequent papers.

In Fig. 11, we have opened a cohesive zone in the spur direction, so that the crack can either branch off its original plane, or emit a dislocation in the spur direction. We call this the Mode I emission configuration. In the figure, we illustrate the branching of the crack. This particular crack will not emit dislocations, but is brittle. In the simulation, the crack was grown to the base of the spur under pure Mode I load, and then a negative Mode II was imposed, and branching occurred for ratio of Mode II to Mode I of 0.4. $\alpha = 0.5$, $\beta = 0.15$. In the figure, we have plotted additional atoms in the linear region above and below the horizontal plane, in order to check that in this complex configuration, the atoms lying in the region of the branch are not violating our assumption that their displacements are in the linear range of the force law. Visual inspection reveals that their displacements are, indeed, small. These additional atoms are all painted black, consistent with the assumption that they lie in the linear portion of the lattice.

One of the special features of this work is the computer time on our Model 35 SGI workstation at 33 MIPS which is required to obtain the results reported above. It required about 20 minutes to construct the perfect lattice Green's functions for the problem as outlined for the Mode II crack, several hours for the Mode I crack, and about 20 minutes to construct the interfacial Green's functions. In each case, about a minute is required to solve the Dyson equation. The final iteration requires from ten seconds to a minute for full convergence ($\simeq 10^{-3}$ lattice spacing)! One should note that once the defect G's are calculated, a large variety of problems can be explored using various force law and loading parameters without calculating new G's. Thus, the realistic time required for making a calculation of a configuration is of the order of a minute. When one realizes that the system we use is very large—4×10^6 atoms in the supercell and crack length of 101 atoms—the power of the method is apparent.

V. CONCLUSIONS.

Detailed discussion of the physical implications of the computer calculations will be presented in subsequent papers. Our purpose here has been to present the basic mathematical background and methodology for making defect calculations in lattices using lattice Green's functions, and to illustrate the methology with calculations in a simple 2D lattice. Crack/dislocation effects are a natural application of the lattice Green's functions, but a variety of other defects, such as defects in grain boundaries, and 3D computations of kinks on cracks and dislocations obviously invite exploration.

The computational speed of the present method, outlined above, is a direct consequence of the procedure of viewing the defect as a perturbation in an otherwise perfect medium. The speed is well beyond that of the other standard techniques for doing quasi-static lattice calculations. For example, in molecular dynamics, a systematic study of crack tip effects such as that we will be reporting in subsequent papers would be a very time consuming, if not impossible task. Although the Green's functions can only be used in static equilibrium situations, activation energies are easily obtained. Further, the sequential intermediate configurations in a relaxation calculation mimic time dependent behavior, if the damping is large. That is, when the forces acting on a configuration are large, the Green's function response is also large, just as in a true time dependent problem. Thus, for example, we learn from our calculations that the dislocation emergence from the crack tip during during the early stages of emission is a slow process, compared with cleavage processes. This effect may turn out to be important in dynamic cracking experiments, where normally brittle materials can cleave if the crack moves fast enough.

ACKNOWLEDGMENTS

The work at Washington University was partly supported by the Department of

Energy under Grant Number DE-FG02-84ER45130.

[1] H. Kanzaki, J. Phys. Chem. Solids, **2**, 24 (1957), *ibid* p. 107.

[2] V. K. Tewary, Adv. Physics, **22**, 757 (1973)

[3] R. Bullough and V. K. Tewary, Dislocations in Solids, ed. F. R. N. Nabarro, Vol. 2, p. 5 North Holland, (1979).

[4] C. Hsieh and R. Thomson, J. Appl. Phys., **44**, 2051 (1973).

[5] R. Thomson, J. Matls. Rsh., **5**, 524 (1990)

[6] K. Masuda-Jindo, V. K. Tewary and R. Thomson, J. Matls. Rsh., **6** (1991).

[7] R. Thomson, V. K. Tewary and K Masuda-Jindo, J. Matls. Rsh., **2**, 619 (1987)

[8] D. Esterling, J. Appl. Phys., **47**, 486 (1976).

[9] V. K. Tewary and R. Thomson, J. Matls. Rsh., in press.

[10] A. Maradudin, E. Montroll, G. Weiss, and I. Ipatova, in Solid State Physics, ed. H. Ehrenreich, F. Seitz and D. Turnbull, Supplement 3, 1971, Academic Press, New York.

[11] P. N. Keating, Phys. Rev. **145**, 637 (1975).

[12] G. F. Koster and J. C. Slater, Phys. Rev. **96**, 1208 (1954).

[13] G. I. Barenblatt, Adv. Appl. Mech., **2**, 55 (1962).

[14] J. Sinclair, Computer Simulation in Physical Metallurgy, ed. G. Jacucci, p 159, ECSC, EEC, EAEC, Brussels, (1986).

[15] D. Kalkstein and P. Soven, Surf. Sci. **26**, 85 (1971).

[16] L. Dobrzynski, S. L. Cunningham, and W. H. Weinberg, Surf. Sci. **61**, 550 (1976).

[17] J. H. Rose, J. R. Smith and J. Ferrante, Phys. Rev., **28**, 1835 (1983).

[18] J. R. Rice and R. Thomson, Phil. Mag. **29**, 73 (1974).

[19] J. R. Rice, J. Mech. Phys. Sol., 40, 239, (1992).

FIGURES

FIG. 1. (a) 2D representation of an infinite periodic lattice. Born–von Karman boundary conditions are assumed with period N in all coordinate directions. (b) A diagram of a lattice with a spring connecting two points in the lattice. A displacement, $u_j(\mathbf{l}')$, of the atom at $\mathbf{l}'$ of in the direction j causes a force, $f_i(\mathbf{l})$ on the atom at $\mathbf{l}$ in the direction i. Springs extend from the reference atom, $\mathbf{l}$, only out to atoms contained within a finite shell surrounding the reference atom.

FIG. 2. Defect sub–space. A set of bonds in the supercell are altered, forming a "defect sub–space" in the lattice. The number of such altered bonds is small compared to the number in the supercell. In the figure, a crack is represented by bond annihilation over a plane constituting the cleavage plane of the crack. Forces, F, are applied to the center of the crack, which provide the load on the crack. At the ends of the crack, a "cohesive zone" is defined over which nonlinear bond forces may be reconstituted, consistent with an assumed force law. Dotted lines in the figure correspond to bonds which have been annihilated, and wavy lines to bonds which have been first annihilated and then reattached with nonlinear bonds.

FIG. 3. Feynman diagram. The term, $\mathbf{G}\delta\Phi\mathbf{G}^*$ in the Dyson equation, (2.7), or (2.8), is analogous to a multiple scattering Feynman diagram with propagators $\mathbf{G}^*$ and $\mathbf{G}$ connected by the scattering operator, $\delta\Phi$. In the diagram, the heavy directed line corresponds to the propagator, $\mathbf{G}^*$, and the light directed line to the propagator, $\mathbf{G}$, while the wavy line corresponds to the $\delta\Phi$. Source and field points, $(\mathbf{l}', \mathbf{l})$, are connected by all possible

intermediate "scattering" events, $\delta\Phi$, corresponding to all the altered bonds of the lattice. When a bond is cut for a two body force, there are two diagrams for each atom of the pair. One diagram, (a), relates to a force generated by displacement in the neighbor, and the second, (b), is the force generated at an atom by its own displacement. The $\delta\Phi$'s for the two are the negative of each other by Newton's third law.

FIG. 4. Interface construction. (a) In an infinite Born–von Karman lattice (represented here in 2D), cuts are made in the xy plane (y direction normal to the page). The cut is repeated in every supercell above and below the original cut, creating a series of disconnected slabs. (b) To form an interface, two slabs with different force constants, $\phi^A(\mathrm{l},\mathrm{l}'), \phi^B(\mathrm{l},\mathrm{l}')$, are reconnected at the cut with a new set of springs, $\phi^{AB}(\mathrm{l},\mathrm{l}')$. The (AB) springs may be different from either slab. In general, the slabs may have different lattice structures, provided they fit at the interface in a periodic manner. Our definition thus encompasses the grain boundary, as well as an interphase boundary.

FIG. 5. Feynman diagrams for slab Dyson equation, (3.1), showing the terms for the bonds annihilated across the upper surface in (a) and (b). These terms are equivalent to Feynman diagrams to the lower surface, as shown in (c) and (d), and are included automatically in the Dyson equation for the periodic structure.

FIG. 6. Feynman diagrams for interface Dyson equation, (3.2). There are terms corresponding only to the reconstructed bonds at the interface.

FIG. 7. A crack in a 2D Hexagonal lattice with nearest neighbor central forces. (a) In

the perfect lattice, the coordinate system for displacements are computed in the rectangular coordinate system, centered on an atom site as shown. For purposes of identifying lattice sites, however, we choose a different coordinate system based on the primitive lattice cell of the hexagonal lattice. (b) The crack is constructed by annihilating bonds between atom sites on top and bottom of a cleavage plane. The crack tip at the left is symmetric to that on the right. A cohesive zone is defined in the vicinity of the right hand tip (but no cohesive zone is constructed at the left tip). As in Fig. 2, dotted lines indicate annihilated bonds, and wavy lines annihilated bonds which have been reattached with nonlinear forces.

FIG. 8. Crack cohesive zone when dislocation emission can occur on a slip plane intersecting the crack, or in which the crack branches onto a different plane. The spur is at 60° to the original cleavage plane.

FIG. 9. Dislocation formation by a crack. The figure shows the cohesive zone (plus one additional atom pair to the left of the cohesive zone). The dislocation is indicated by the vertical orientation of the atoms in the core, which corresponds to a horizontal relative displacement of half a lattice spacing. The atoms are represented by the filled circles centered at the atom positions, whose radius is the radius of the atom in the lattice, and with a gray scale color which varies from full black to full white. Full black corresponds to zero force exerted on the atom from atoms across the cleavage plane, and full white represents the maximum force which can be exerted by the universal binding relation. An additional circle centered at the atom position indicates the range of the force law. Note that on the left, the range circles for the completely black atoms do not touch their neighbors on the opposite cleavage plane. The cohesive zone overlapped by the dislocation core is indicated by the nearly white atoms, and the increasingly black atoms to the right indicates

the decreasing elastic stress.

FIG. 10. Dislocation emission from a crack on an interface. With the same size crack and cohesive zone as in Fig. 9, a crack is formed in the cohesive zone, and then emits under Mode II. In this case, the interfacial bonding is weaker than in Fig. 9, and the dislocation core is much broader. Note the unsymmetric displacements in the upper cleavage plane relative to the lower.

FIG. 11. Branching of a crack. The crack length is the same as in Fig. 9, (but with the cohesive zones shown). Because of the spur in the cohesive zone, relaxations can occur on one plane outside the normal cleavage plane. In the same way as in Fig. 9 , after an equilibrium crack is formed in the cohesive zone at the spur base, under negative Mode II loads, the crack cleaves on the spur cleavage plane.

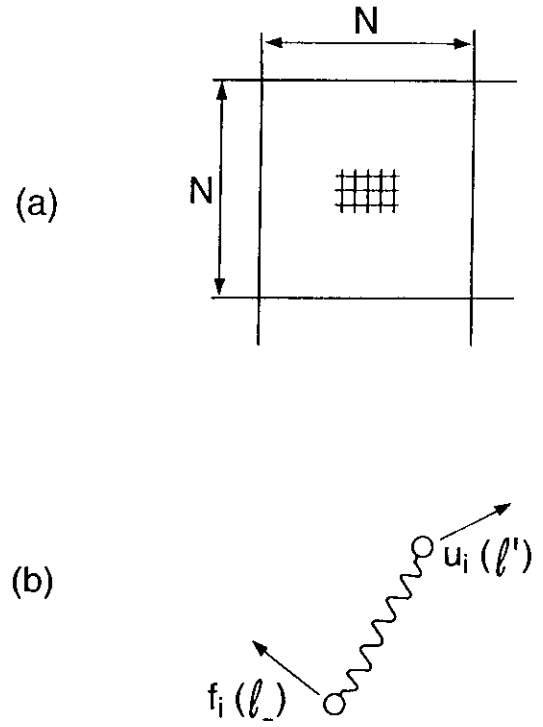

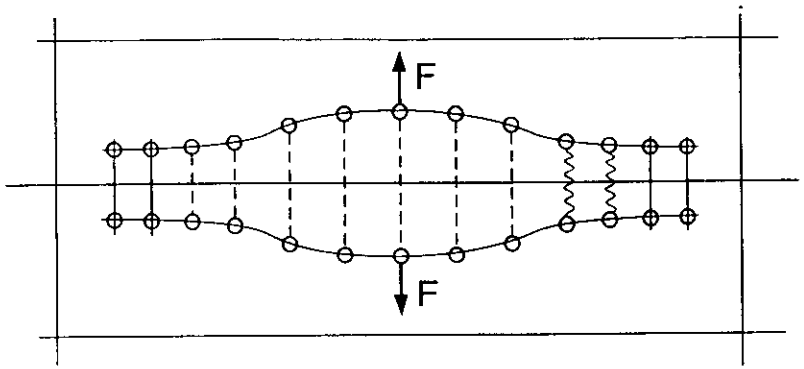

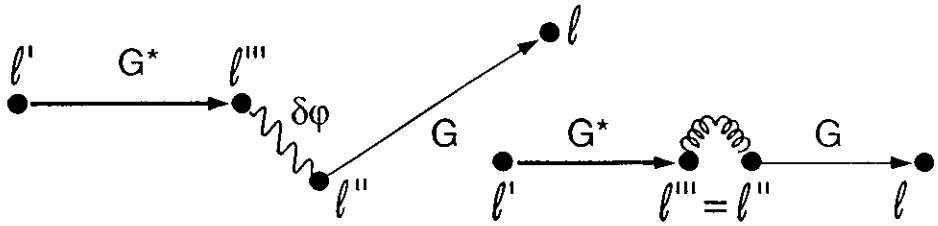

(a) (b)

Fig. 4

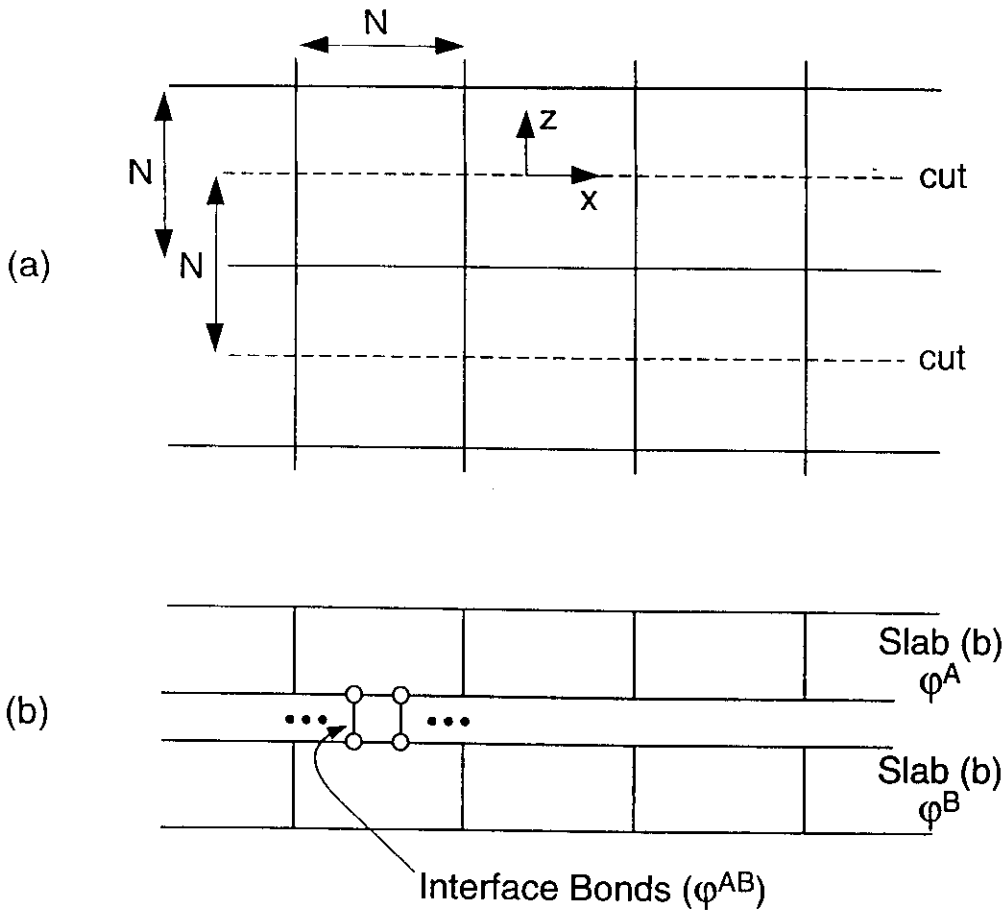
(a)
N
N
N
z
x
cut
cut
(b)
Slab (b)
φ^A
Slab (b)
φ^B
Interface Bonds (φ^{AB})

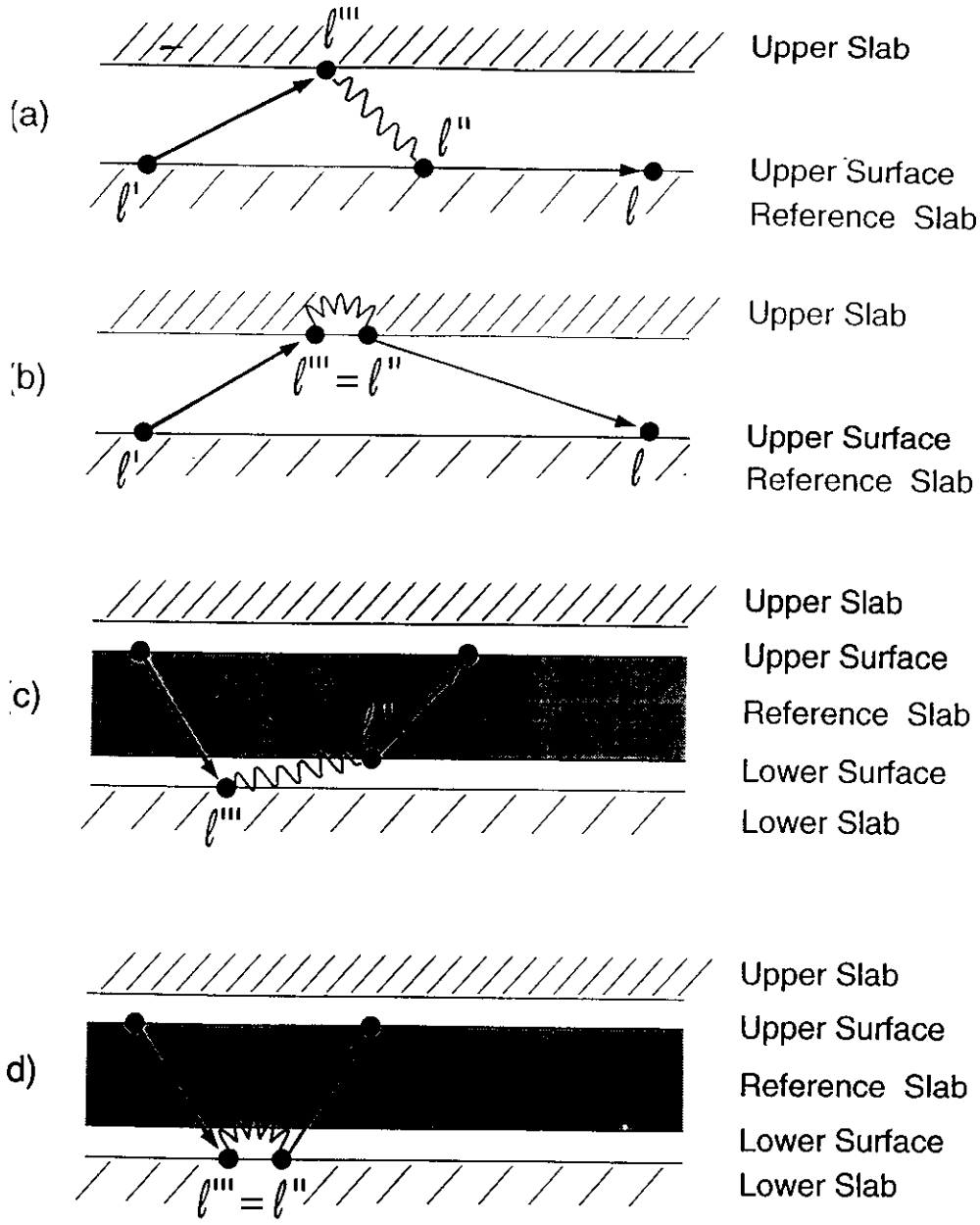
(a)
ℓ'''
ℓ''
ℓ'
ℓ
Upper Slab
Upper Surface
Reference Slab
(b)
$\ell''' = \ell''$
ℓ'
ℓ
Upper Slab
Upper Surface
Reference Slab
c)
ℓ'''
Upper Slab
Upper Surface
Reference Slab
Lower Surface
Lower Slab
d)
$\ell''' = \ell''$
Upper Slab
Upper Surface
Reference Slab
Lower Surface
Lower Slab

Fig. 7

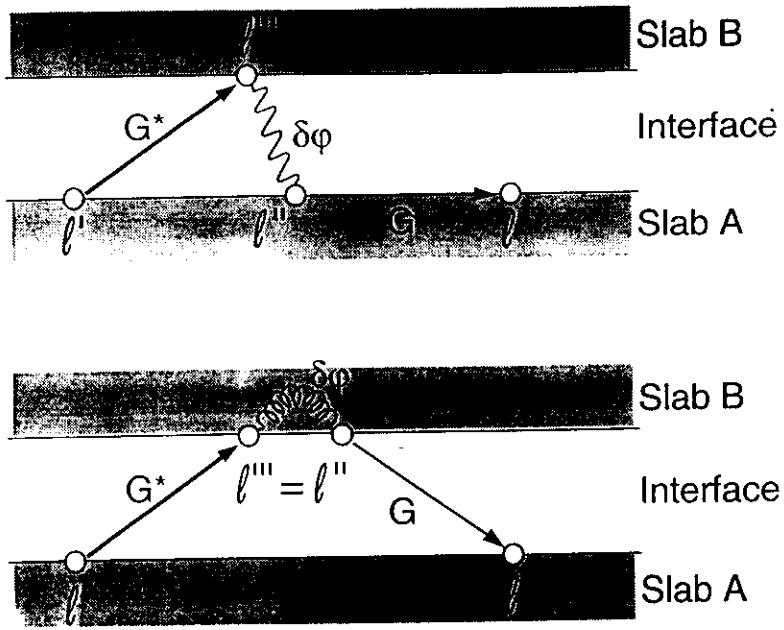
Slab B
Interface
Slab A
G*
δφ
G
Slab B
Interface
Slab A
G*
G

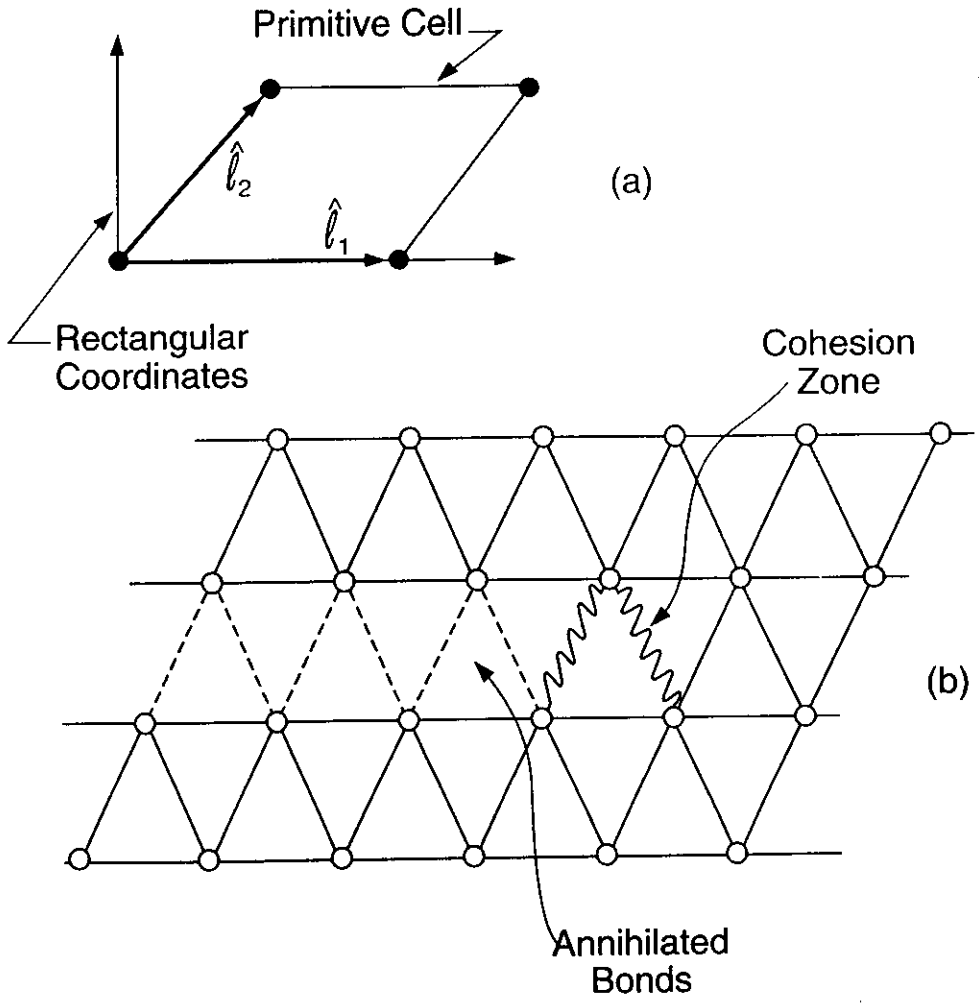
Primitive Cell
(a)
Rectangular Coordinates
Cohesion Zone
(b)
Annihilated Bonds